

# COMPUTATIONAL MODELING OF THE TRAILMASTER PROCYON SYSTEM\*

A. E. Greene, R. L. Bowers, J. H. Brownell, J. H. Goforth  
H. Oona, D. L. Peterson, D. G. Rickel, D. L. Weiss

Los Alamos National Laboratory  
P.O. Box 1663  
Los Alamos, NM 87544

## I. Introduction

The goal of the Los Alamos Foil Implosion project (Trailmaster) is the development of an intense source of soft x-rays for materials and fusion studies. The x-ray source in the Trailmaster project is a foil initiated z-pinch. The next system in the Trailmaster project is designed to deliver 15 MA of current to the imploding liner creating approximately 1 MJ of soft x-ray radiation in a submicrosecond pulse. This system, designated Procyon, will consist of a Mark IX helical explosive generator, an explosively formed fuse (EFF) opening switch, detonator closing switches, a vacuum powerflow channel, a plasma flow switch (PFS), and the imploding foil load.

Companion papers at this conference will discuss the status of subsystem experiments leading up to the Procyon system,<sup>1,2</sup> Procyon diagnostics,<sup>3</sup> and details of MHD simulations of the plasma flow switch.<sup>4</sup> In the present paper we will focus on the computational modeling of the overall Procyon system. This effort includes circuit and zero-dimensional point mass (slug) modeling, 1-D and 2-D radiation MHD calculations, and 3-D radiation transport and view factor modeling of the vacuum powerflow channel.

## II. Circuit and 0-D Calculations

A conceptual diagram of the Procyon system is shown in Figure 1. The equivalent electrical circuit for this system is shown in Figure 2. The Los Alamos firing point 88 capacitor bank and the Mark IX generator have both been documented in previous publications.<sup>5,6</sup> The EFF in the Procyon system is being fielded in a flux conserving geometry<sup>1</sup> in which the inductance of the switch remains in the circuit after the switch opens. This is the 57 nH storage inductor in Figure 2. Based on projections from small scale experiments and early Procyon subsystem experiments<sup>1</sup>, we are modeling the resistance as a function of time for this switch with the curve shown in Figure 3.

With a seed current of 450 kA from the capacitor bank we calculate that the Mark IX generator will deliver some 23 MA into this system as shown in Figure 4. Note, however, that between the capacitor bank discharge and the generator run the build up of the current requires some 340  $\mu$ s. Hence the need for pulse shaping prior to driving the plasma flow switch and imploding load.

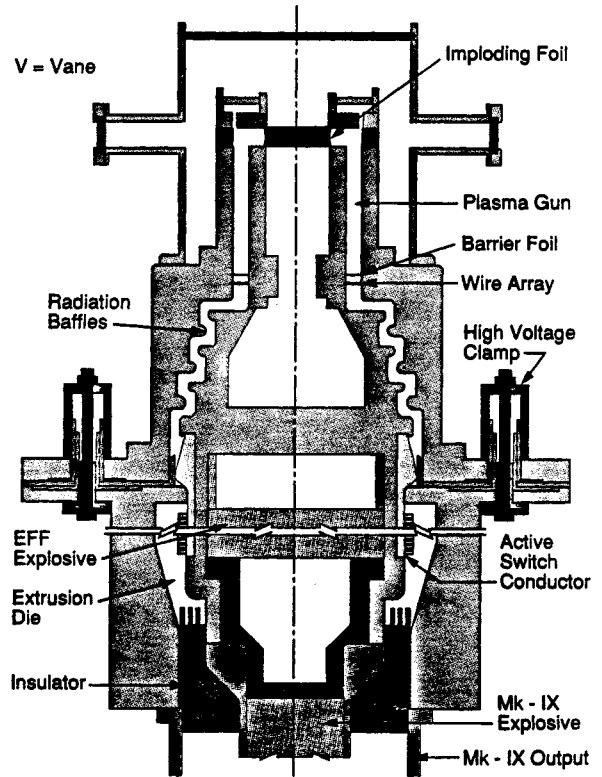


Fig. 1 Diagram of the Procyon system.

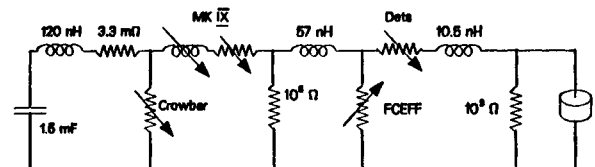


Fig. 2 Equivalent circuit for the Procyon system. (The  $10^3 \Omega$  resistor in vertical branch 4 is for computational purposes and is large enough to prevent current flow but small enough to permit accurate voltage calculations at the vacuum interface.)

\*Work performed under the auspices of the University of California for the US Department of Energy under contract number W-7405-ENG- 36.

# Report Documentation Page

*Form Approved*  
*OMB No. 0704-0188*

Public reporting burden for the collection of information is estimated to average 1 hour per response, including the time for reviewing instructions, searching existing data sources, gathering and maintaining the data needed, and completing and reviewing the collection of information. Send comments regarding this burden estimate or any other aspect of this collection of information, including suggestions for reducing this burden, to Washington Headquarters Services, Directorate for Information Operations and Reports, 1215 Jefferson Davis Highway, Suite 1204, Arlington VA 22202-4302. Respondents should be aware that notwithstanding any other provision of law, no person shall be subject to a penalty for failing to comply with a collection of information if it does not display a currently valid OMB control number.

1. REPORT DATE <b>JUN 1991</b>	2. REPORT TYPE <b>N/A</b>	3. DATES COVERED <b>-</b>			
4. TITLE AND SUBTITLE <b>Computational Modeling Of The Trailmaster Procyon System</b>		5a. CONTRACT NUMBER			
		5b. GRANT NUMBER			
		5c. PROGRAM ELEMENT NUMBER			
6. AUTHOR(S)		5d. PROJECT NUMBER			
		5e. TASK NUMBER			
		5f. WORK UNIT NUMBER			
7. PERFORMING ORGANIZATION NAME(S) AND ADDRESS(ES) <b>Los Alamos National Laboratory P.O. Box 1663 Los Alamos, NM 87544</b>		8. PERFORMING ORGANIZATION REPORT NUMBER			
9. SPONSORING/MONITORING AGENCY NAME(S) AND ADDRESS(ES)		10. SPONSOR/MONITOR'S ACRONYM(S)			
		11. SPONSOR/MONITOR'S REPORT NUMBER(S)			
12. DISTRIBUTION/AVAILABILITY STATEMENT <b>Approved for public release, distribution unlimited</b>					
13. SUPPLEMENTARY NOTES <b>See also ADM002371. 2013 IEEE Pulsed Power Conference, Digest of Technical Papers 1976-2013, and Abstracts of the 2013 IEEE International Conference on Plasma Science. Held in San Francisco, CA on 16-21 June 2013. U.S. Government or Federal Purpose Rights License</b>					
14. ABSTRACT					
15. SUBJECT TERMS					
16. SECURITY CLASSIFICATION OF:			17. LIMITATION OF ABSTRACT <b>SAR</b>	18. NUMBER OF PAGES <b>4</b>	19a. NAME OF RESPONSIBLE PERSON
a. REPORT <b>unclassified</b>	b. ABSTRACT <b>unclassified</b>	c. THIS PAGE <b>unclassified</b>			

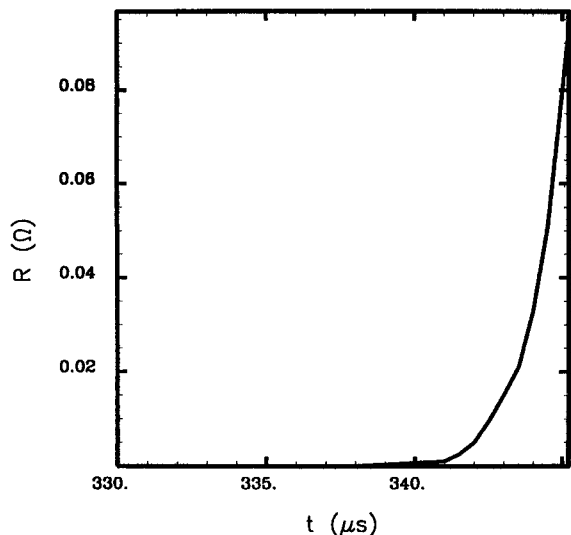


Fig. 3 Time dependent resistance of the explosively formed fuse during opening.

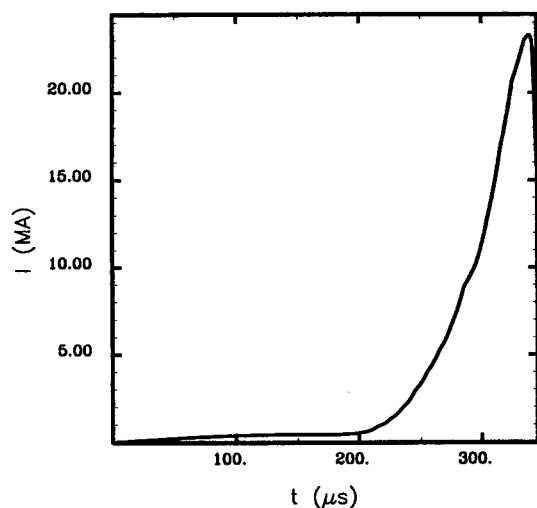


Fig. 4 Calculated current from the Mark IX generator into the storage inductor.

The time dependent resistance in horizontal branch 4 of the circuit represents the detonator closing switches. The total resistance of the six switches in parallel drops to  $0.3 \text{ m}\Omega$  in about  $1 \mu\text{s}$ .

Current transferred to the plasma flow switch depends to some extent on the design of the switch itself and details of the Procyon design are not yet finalized. The switch used for the calculations presented here has an inner electrode radius of  $7.6 \text{ cm}$ , outer electrode radius of  $10.2 \text{ cm}$  and a total switch mass of  $150 \text{ mg}$ . The distance from the center of mass of the wire array plus barrier foil (which merge to form the switch plasma) to the upstream side of the  $2 \text{ cm}$  long load slot is  $6.5 \text{ cm}$ . Our calculations indicate that the system described above will deliver  $15 \text{ MA}$  of current to this plasma flow switch by the time it reaches the load slot (see Figure 5).

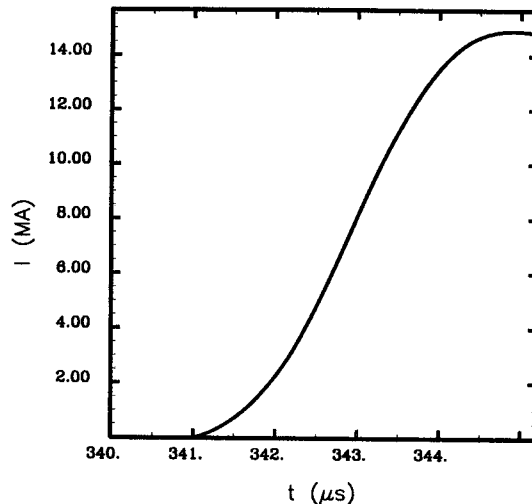


Fig. 5 Calculated current transferred to the plasma flow switch.

The radiation output from this system will depend on the switching efficiency of the PFS, the mass and geometry of the imploding load, and the quality of the implosion. These are all issues that are being addressed by experiments and calculations at the present time. A simple slug model calculation of the implosion of the load fielded in the previous shot series (a  $250 \text{ nm}$  thick,  $2 \text{ cm}$  long,  $5 \text{ cm}$  radius, unbacked aluminum foil) driven by this system with a final implosion ratio of  $10:1$  predicts a kinetic energy of  $750 \text{ kJ}$ ; essentially all of which will be converted to radiation. However, with the lower inductance power flow channel shown in section V this system will deliver more than  $16 \text{ MA}$  to the plasma flow switch. With that current level it is easy to design an imploding load for which slug model calculations predict more than  $1 \text{ MJ}$  of kinetic energy.

### III. 1-D Plasma Flow Switch Calculations

We are using the 1-D, radiation MHD code, RAVEN, in planar geometry to provide radiation flux estimates and initial conditions for 2-D, Eulerian, calculations. The 1-D calculations permit us to model, at least to some approximation, the initiation of the aluminum, its assembly on the barrier foil, and the total switch plasma's run down the coaxial barrel. We have used the radiated flux estimates from these calculations to estimate the extent to which the vacuum powerflow channel may close due to radiative induced ablation<sup>7</sup> (see also section V below).

In 1-D we simulate the wire array as a  $55.86 \text{ cm}$  wide by  $2.54 \text{ cm}$  long, solid density, aluminum foil that is  $1.94 \mu\text{m}$  thick. The barrier foil is modeled as a  $3.78 \mu\text{m}$  thick polyurethane foil. This gives a total mass of  $150 \text{ mg}$ . The equations-of-state for these calculations are taken from the Los Alamos SESAME tables.

The calculated positions of the Lagrangian zones as functions of time are shown in Figure 6. Note that this calculation predicts that the plasma will reach a maximum expansion of 1.5 cm before the expansion due to the explosion of the foil is overcome by the  $j \times B$  force (the slight expansion of the barrier foil is due to a small positive pressure from the EOS table at the initial conditions which is slightly above room temperature). The plasma will reach the location of the imploding load slot in almost exactly 4  $\mu s$ . At that time the 1-D simulation predicts a thickness of the current carrying sheath to be 0.4 cm. After 4  $\mu s$  the fastest zones are moving at 7.3 cm/ $\mu s$  and the slowest at 6.5 cm/ $\mu s$ .

The calculated temperatures as functions of time are shown in Figure 7. The temperature peaks are each associated with internal compressions within the plasma. These compressions start when the back of the aluminum plasma overtakes the front which has been slowed by the collision between the aluminum and the polyurethane. The 1-D calculations indicate that the maximum temperatures occur on the back (upstream) side of the aluminum plasma rather than at the boundary between the aluminum and the barrier foil.

#### IV. 2-D Plasma Flow Switch Calculations

More details concerning the PFS calculations are available in the companion paper by Peterson et al. Figure 8 shows a 2-D, Eulerian, Procyon, PFS calculation near the point at which material and field begin to enter the load slot. In this calculation the load is a 5 cm radius copper rod. We are, therefore, just calculating the efficiency with which this switch will deliver current to the position of the load,  $r=5$  cm. This calculation was driven by the  $I(t)$  curve shown in Figure 5 above. The calculation was started 2  $\mu s$  after the current reaches the wire array which is approximately the point of maximum expansion shown in Figure 6. In this calculation the 150 mg plasma was treated as all Al. It was given an expansion of 1.5 cm in the  $z$  direction, a uniform temperature of 1 eV, and a  $1/r^2$  density distribution.

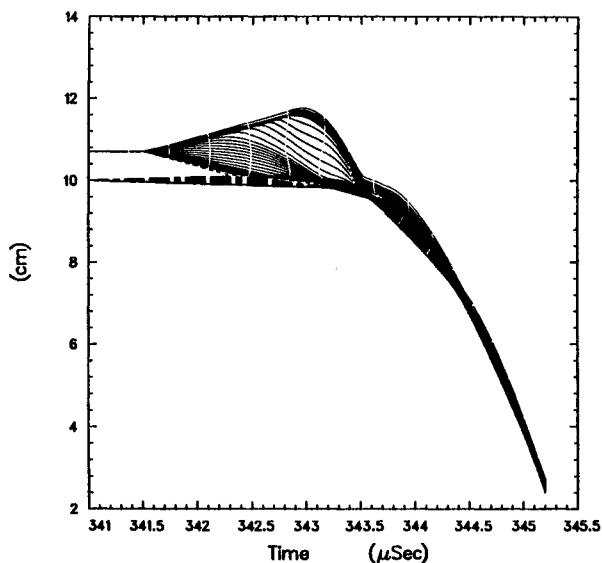


Fig. 6 Positions of the Lagrangian zones in the 1-D planar plasma flow switch calculation.

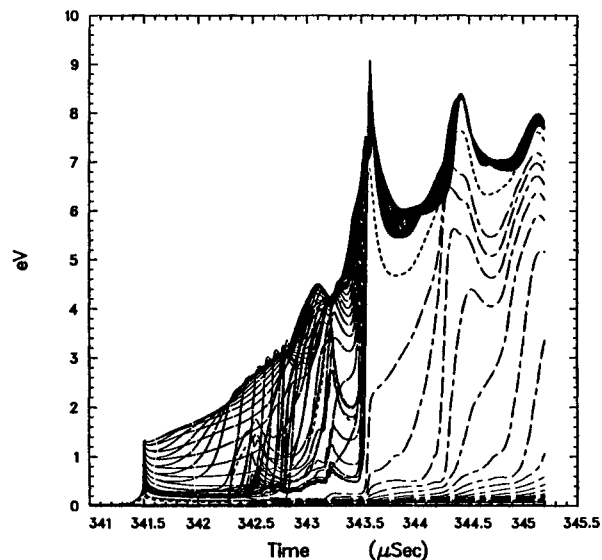


Fig. 7 Temperatures of the Lagrangian zones in the 1-D plasma flow switch calculation.

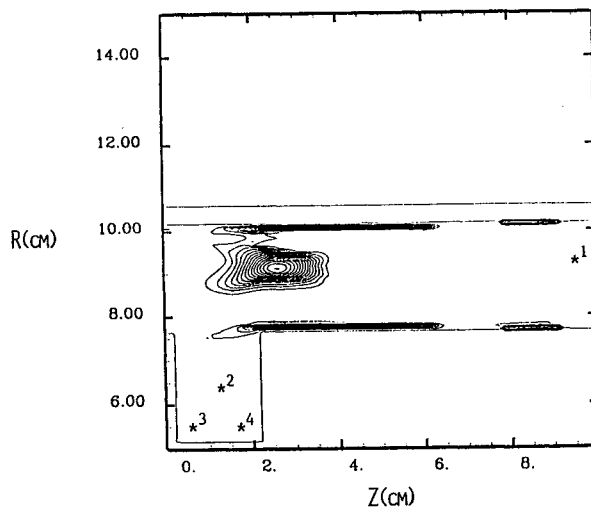


Fig. 8 Density contours in the 2-D calculation at 4  $\mu s$ . Minimum density shown is  $1.0 \times 10^{-4}$  gm/cm<sup>3</sup>. Starred points were edited to provide figure 9 values.

Figure 9 shows calculated time dependent current traces for the positions indicated in Figure 8 during switching. The calculated values in the load slot oscillate above and below the feed value (curve 1) because the magnetic field is being compressed as the switch material carrying it encounters the fixed inner electrode in the load slot. The curves have settled by 4.7  $\mu s$  (2.7  $\mu s$  after the start of the calculation) to values quite close to the feed value. The slow, 0.2 to 0.4  $\mu s$  rise times indicate that these currents are being carried into the load slot by a significant amount of switch material. Indeed, in this calculation some 4 mg of switch mass was deposited into the load slot. This is essentially the same as the mass of the load described in section II. We are presently exploring a variety of options for reducing the mass deposited while maintaining switching efficiency.

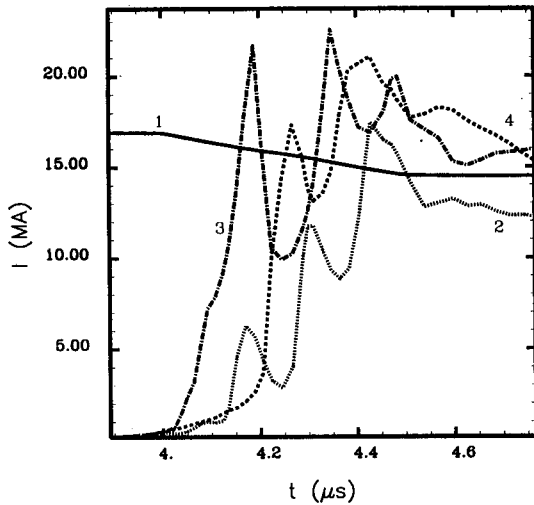


Fig. 9 Calculated time dependent current profiles at locations marked in figure 8.

### V. 3-D View Factor Calculations

Our 3-D radiation transport and view factor code has been benchmarked against the measured radiation attenuation of the vacuum powerflow channel shown in Figure 1. We find that with an average surface albedo of 0.35 for the anodized surfaces, radiation emitted from the initial position of the wire array is attenuated by a factor (output/input) of  $1.6 \times 10^{-8}$ . Our 1-D calculation provides an estimate of  $1.1 \times 10^2$  J/cm<sup>2</sup> radiated toward the vacuum interface. Therefore, we expect about  $1.8 \mu\text{J}/\text{cm}^2$  to reach the interface through the present channel, almost surely a safe level.<sup>8</sup>

### References

1. J. H. Goforth, H. Oona, J. H. Brownell, A. E. Greene, H. W. Kruse, I. R. Lindemuth, S. P. Marsh, J. V. Parker, R. E. Reinovsky, D. G. Rickel, and P. J. Turchi, "Procyon Experiments Utilizing Explosively-Formed Fuse Opening Switches," to be presented at the 8th IEEE Pulsed Power Conference, San Diego CA, June 17-19, 1991.
2. D. G. Rickel, I. R. Lindemuth, R. E. Reinovsky, J. H. Brownell, J. H. Goforth, A. E. Greene, H. W. Kruse, H. Oona, J. V. Parker, and P. J. Turchi, "Procyon Experiments Utilizing Foil-Fuse Opening Switches," *ibid.*
3. H. Oona, B. G. Anderson, C. E. Findley, J. H. Goforth, A. E. Greene, H. W. Kruse, J. V. Parker, and D. G. Rickel, "Plasma and Electrical Diagnostics for Procyon Experiments," *ibid.*
4. D. L. Peterson, R. L. Bowers, A. E. Greene, J. H. Brownell, and N. F. Roderick, "Computational Simulations of Plasma Flow Switches and Imploding Loads," *ibid.*

Figure 10 shows a greatly reduced powerflow channel which we calculate to have about 8.5 nH of inductance. Our view factor calculations indicate that this revised channel can provide essentially the same level of attenuation if the average surface albedo of the double lined surfaces can be reduced to 0.1. This will require the actual removal of material from these surfaces to provide radiation traps. Experiments on this approach are now in progress.

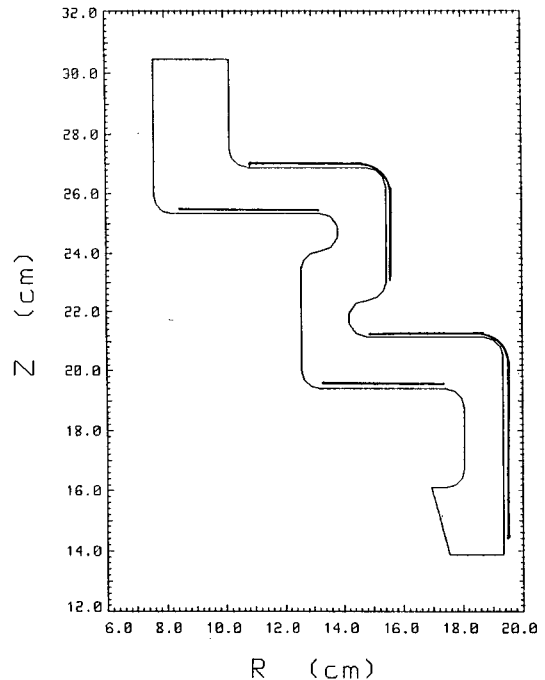


Fig. 10 Diagram of a reduced inductance vacuum powerflow channel. Double lines indicate walls which must have albedoes reduced to 0.1 by removal of material.

5. D. J. Erickson, B. L. Freeman, J. E. Vorthman, R. S. Caird, C. M. Fowler, J. C. King, A. R. Martinez, J. V. Repa, J. B. VanMarter, and R. G. Vaughn, "Firing Complex for Explosive Pulsed Power," Proceedings of the Fourth International Conference on Megagauss Magnetic Field Generation and Related Topics, p353, Santa Fe NM, July 14-17, 1986.
6. C. M. Fowler and R. S. Caird, "The Mark IX Generator," Digest of Technical Papers, Seventh IEEE Pulsed Power Conference, p475, Monterey CA, June 11-14, 1989.
7. A. E. Greene, R. L. Bowers, T. A. Oliphant, D. L. Peterson, and D. L. Weiss, "Calculational Evaluation of Plasma Flow Switches for the Los Alamos Foil Implosion Project," *ibid.* p699.
8. C. Enloe, R. Blaher, M. Coffing and R. E. Reinovsky, "Vacuum Ultra-Violet Effects on power Transport Across a Vacuum/Solid dielectric Interface," Proceedings: Tenth International Symposium on discharges and Electrical insulation in Vacuum, p 308, Columbia SC, Oct. 25-28, 1982.